Halloysite Nanotubes as Particulate Emulsifier: Preparation of Biocompatible Drug-Carrying PLGA Microspheres Based on Pickering Emulsion

Zengjiang Wei, Chaoyang Wang, Hao Liu, Shengwen Zou, Zhen Tong

Research Institute of Materials Science, South China University of Technology, Guangzhou 510640, China

Received 31 August 2011; accepted 7 November 2011
DOI 10.1002/app.36456
Published online 17 January 2012 in Wiley Online Library (wileyonlinelibrary.com).

ABSTRACT: Halloysite nanotubes (HNTs)-coated micrometer-sized poly(lactic-coglycolic acid) (PLGA) microparticles were fabricated via a combined system of "Pickering-type" emulsion route and solvent volatilization method in the absence of any molecular surfactants. Stable oil-in-water emulsions were prepared using HNTs as a particulate emulsifier and a dichloromethane (CH_2Cl_2) solution of PLGA as an oil phase. The HNTs-coated PLGA microparticles were fabricated by the evaporation of CH_2Cl_2 from the emulsion, and then bare-PLGA microparticles were prepared by removal of the HNTs. SEM with energy dispersive analysis system (EDS) study confirmed adsorption of the HNTs only at the surface of the PLGA microparticles. After washing with acid aqueous solution, there is negligibly small amount of HNTs on the bare-PLGA microparticles. Moreover, ibuprofen (IBU) as a drug model was loaded into the bare-PLGA microparticles. And, the release curves were nicely fitted by the Weibull equation and the release followed Fickian diffusion. The combined system of Pickering emulsion and solvent volatilization opens up a new route to fabricate a variety of microparticles. © 2012 Wiley Periodicals, Inc. J Appl Polym Sci 125: E358–E368, 2012

Key words: pickering emulsion; microparticles; PLGA; halloysite nanotubes; biocompatible

INTRODUCTION

Biodegradable synthetic polymers have been used in the fields of drug-carrier and reconstructive surgery[1] because they do not need to be removed after healing. Biodegradable synthetic polymers have also been used in tissue engineering as a physical support for cells to enable cell adhesion, proliferation, differentiation, and tissue regeneration.[2,3] Biodegradable microparticles have attracted considerable attention for their unusual properties, which suggest a number of applications including microencapsulation and even scaffolds for tissue engineering applications.

Correspondence to: C. Wang (zhywang@scut.edu.cn).

Contract grant sponsor: National Basic Research Program of China; contract grant number: 973 Program, 2012CB821500.
Contract grant sponsor: NSFC; contract grant numbers: 20874030, 50973034.
Contract grant sponsor: Fundamental Research Funds for the Central Universities.
Contract grant sponsor: The Planned Science and Technology Project of Guangdong Province; contract grant number: 2010B010800017.
Contract grant sponsor: PCSIRT; contract grant number: IRT0827.

Recently, self-assembly of nanoparticles at liquid–liquid interfaces has been well documented and offers a straight forward pathway for the production of organized nanostructures.[4] In this approach, nanoparticles spontaneously localize at the interface to minimize the helmholtz free energy. Typically, hydroxyapatite nanocrystal-coated PLLA microspheres have been successfully prepared by the Pickering emulsion method.[5,6] Pickering emulsions are solid particle-stabilized emulsions in the absence of any molecular surfactant, where solid particles adsorbed to an oil-water interface.[7,8] Although this area of research lay dormant for many years, there has been increasing interest recently. The solid particles used in Pickering emulsions can be silica[9,10] metals,[11,12] cellulose,[13] apatite,[14,15] clays,[16–19] microgels,[20] and polystyrene latexes.[21,22] The wetability of the particulate emulsifiers to oil-water interfaces decides the stability and type of emulsions.

Halloysite nanotubes (HNTs) have been developed as an entrapment system for loading, storage, and controlled release of anticorrosion agents and biocides.[23] And, HNTs are available in thousands of tons, and remain sophisticated and novel natural nanomaterials which can be used for the loading of agents for metal and plastic anticorrosion and biocide protection.[24] To the best of our knowledge, HNTs as a particulate emulsifier was firstly reported in Pickering emulsion. In this study, we report the

TABLE I
Comparison of HNTs with CNTs

Items	Halloysite nanotubes	Carbon nanotubes
Inner diameter	15 nm	2 nm
Length	ca. 1000 nm	ca.1000 nm
Biocompatibility	Good	Toxic
Price	ca. 4 $ per kg	ca. 500 $ per kg
Supply level	Available in thousands of tons	Gram

preparation of CH_2Cl_2 emulsion droplets with the HNTs by dissolving PLGA in CH_2Cl_2. As a polymer, PLGA was used in this study, which is certificated by Food and Drug Administration (FDA, USA) and have been used in the fields of orthopedic and reconstructive surgery[25] and tissue engineering[26] because it is not necessary to remove the polymeric materials after healing. Next, we describe the synthesis of HNTs-coated PLGA microparticle by the evaporation of the oil from the CH_2Cl_2 solution of PLGA-in-water emulsions. Then, the bare-PLGA microparticle (biodegradable microparticle) was prepared by removal HNTs from HNTs-coated PLGA microparticle using acid aqueous solution. Finally, ibuprofen (IBU) as a model drug is loaded into the PLGA microparticle by dispersing in water phase during the microparticle fabrication process. The release behavior of the drug-loaded microparticle was investigated. By comparing the spectra with time, the release profile of IBU at different conditions had been evaluated.

The synthetic method described in this study needs neither molecular surfactant nor polymeric stabilizer, which is usually used to synthesize/stabilize the microparticle in media and has possibilities to cause allergy-like reactions and carcinogenicity[27] at the same time. In this study, there is only biodegradable PLGA remaining in the result of microparticle. To the best of our knowledge, this is the first report of the preparation of PLGA microparticles using HNTs based on a combined system of Pickering emulsion and solvent volatilization. In addition, HNTs is a common mineral resource, which is cheaper than other nanotubes, such as carbon nanotubes (CNTs).[28] Compared with CNTs, HNTs has many advantages illustrated in Table I.[23] This fabrication technique provides a facile way to create new biocompatible beads with matrix of bioactive PLGA for biomedical applications. It is expected to be a potential candidate in microparticle engineering and drug-carrying system.

EXPERIMENTAL

Materials

The HNTs, mined from Yichang, Hubei, China, were purified according to.[29] A typical procedure is described below. A 10 wt % water solution of halloysite was prepared by slow addition of water to dry halloysite. Then 0.05 wt % sodium hexametaphosphate was added to the solution while stirring. The solution was stirred for 30 min and left to stand for 20 min at room temperature. The clay aggregate and impurities were precipitated in the bottom and were removed by filtration. The upper solution was carefully collected and the resulting HNTs were separated by centrifugation and dried at 80°C in air for 5 h. Dichloromethane (CH_2Cl_2), 55% hydrogen fluoride aqueous solution, 36% hydrochloric acid aqueous solution, methanol were bought from Guangzhou Chemical Factory (China) and were used without further purification. PLGA was purchased from Shandong Medical Instrument Research Institute (China). The water used in all experiments was purified by deionization and filtration with a Millipore purification apparatus to a resistivity higher than 18.0 MΩ cm.

Fabrication of HNTs-stabilized emulsion

The aqueous dispersions of the HNTs with a solid content (0.5 wt %) were prepared by adding 0.05 g HNTs to 10 mL water. And then, these dispersions were deoxygenated by bubbling through nitrogen gas for 10 min and dispersed by ultrasonic at room temperature in the dark place. Finally, 2 mL CH_2Cl_2 solution of PLGA (2.0% solid contents) as the oil phase was added to the aqueous phase and the system was emulsified by hand-shaking for 5 min. This fabrication strategy was illustrated in part of Figure 1.

Fabrication of HNTs-coated PLGA and bare-PLGA microparticle

The HNTs-coated PLGA microparticles were prepared via in situ evaporation of CH_2Cl_2 from the emulsion at 39°C for 48 h. Meanwhile, the emulsion packing in an open vial was slightly shaken by a mechanical vibrator. At the end of the evaporation of CH_2Cl_2, the resulting microparticles were purified by three centrifugation/redispersion cycles, replacing each decanted supernatant with deionized water. Bare-PLGA microparticles were prepared by removal of the HNTs from the HNTs-coated PLGA microparticle using mixture aqueous solution of HF and HCl, which can dissolve the HNTs component. These bare-PLGA microparticles were used after washing with deionized water to remove ionic species generated by dissolution of the HNTs. The bare-PLGA microparticles were purified by centrifugation/redispersion process, replacing each successive supernatant with pure water, and followed by drying overnight in a vacuum at 45°C for 12 h. The final product was white powder. This fabrication strategy was illustrated in part of Figure 1.

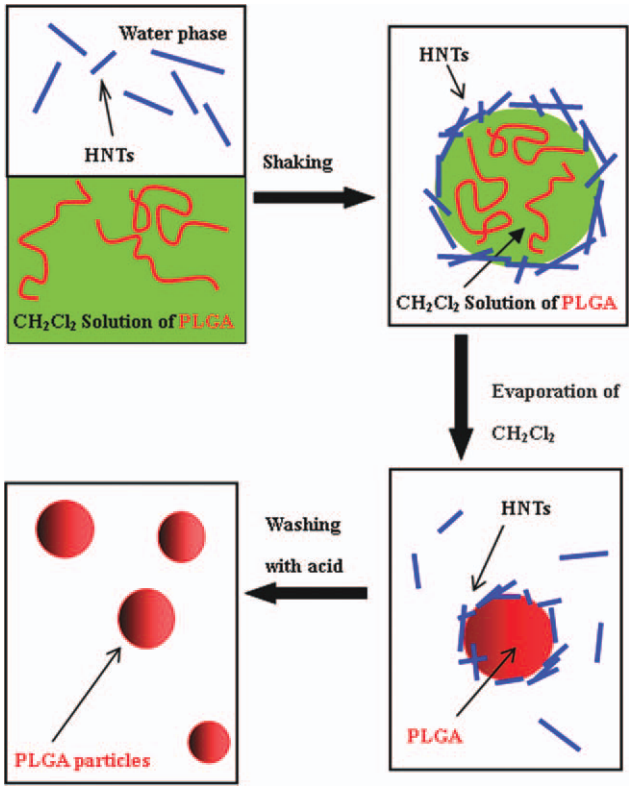

Figure 1 Schematic illustration of the preparation of HNTs-coated PLGA microspheres and bare-PLGA microparticles by evaporation of solvent based on Pickering emulsion droplets. [Color figure can be viewed in the online issue, which is available at wileyonlinelibrary.com.]

Determination of IBU loading capacity and encapsulation efficiency

Drug-loaded PLGA microspheres were fabrication in the same way as described above (10 mL aqueous dispersions of the HNTs, HNTs, 0.5%, wt %; 2 mL PLGA-CH_2Cl_2 solution, PLGA, 2%, wt %) except that CH_2Cl_2 solution of PLGA contained different amounts of IBU (drug: copolymer, 7.5–30%, wt %) in the PLGA microparticles fabrication process (shown in Table II). Drug-loaded bare-PLGA microparticles were prepared by removal of the HNTs from the HNTs-coated PLGA microparticles by adding mixed acid aqueous solution. And then, the supernatant in the cycles of purification were collected by centrifugation for 10 min at 8000 rpm. The concentration and volume of supernatant was used for analysis of IBU in bare-PLGA microparticles. The unencapsulated IBU quantity of IBU was estimated on the basis of the fluorescence intensity at 232 nm of the supernatant solution by an ultraviolet and visible spectrophotometer. Loaded content was determined using the calibration curve established from standard solutions of IBU in acid aqueous solution. Each experiment was carried out in triplicate, and mean values were calculated using the following formulas:

$$\text{Drug loading capacity (DL \%)}$$

$$\mathrm{DL\%} = \left(\frac{\text{Weight of drug in PLGA particles}}{\text{Weight of PLGA particles}}\right) \times 100\% \quad (1)$$

$$\text{Encapsulation efficiency (EE \%)}$$

$$\mathrm{EE\%} = \left(\frac{\text{Weight of drug in PLGA particles}}{\text{Weight of feed drug}}\right) \times 100\% \quad (2)$$

In vitro release experiment

In this *in vitro* drug release experiment, 25 mg drug-loaded PLGA microspheres powder was dispersed into 20 mL PBS solution. The dispersion was transferred into a dialysis bag (cut off molecular weight 7000 g/mol). And then, the dialysis bag was immersed into 180 mL of PBS solution with different pH value (pH = 1.2 or 7.4) at 37°C with magnetic stirring in a three-necked flask (capacity: 250 mL). An amount of 2.0 mL of solution was withdrawn at a predetermined time interval. The amount of released drug was measured by a UV–vis spectrophotometer at 232 nm. After UV-test, 2.0 mL of solution was poured back into the three-necked flask. The cumulative released quantity can be evaluated constantly with UV spectroscopy intensity. The relationship between fluorescence intensity and

TABLE II
Summary of O/W Emulsions Formed Using Different Parameter

No.	(Drug: PLGA, m/m) (%)	pH	PLGA in CH_2Cl_2 (wt %)	Encapsulation efficiency (%)	Drug loading capacity(%)
1	7.5	1	2%	81.64	5.77
2	7.5	3	2%	79.84	5.65
3	7.5	5	2%	78.01	5.51
4	7.5	7.2	2%	76.51	5.42
5	15	7.2	2%	91.17	12.03
6	30	7.2	2%	96.11	22.38
7	30	1.2	2%	97.83	29.35

Each data point in this table is represents the average of three tests, ($n = 3$).

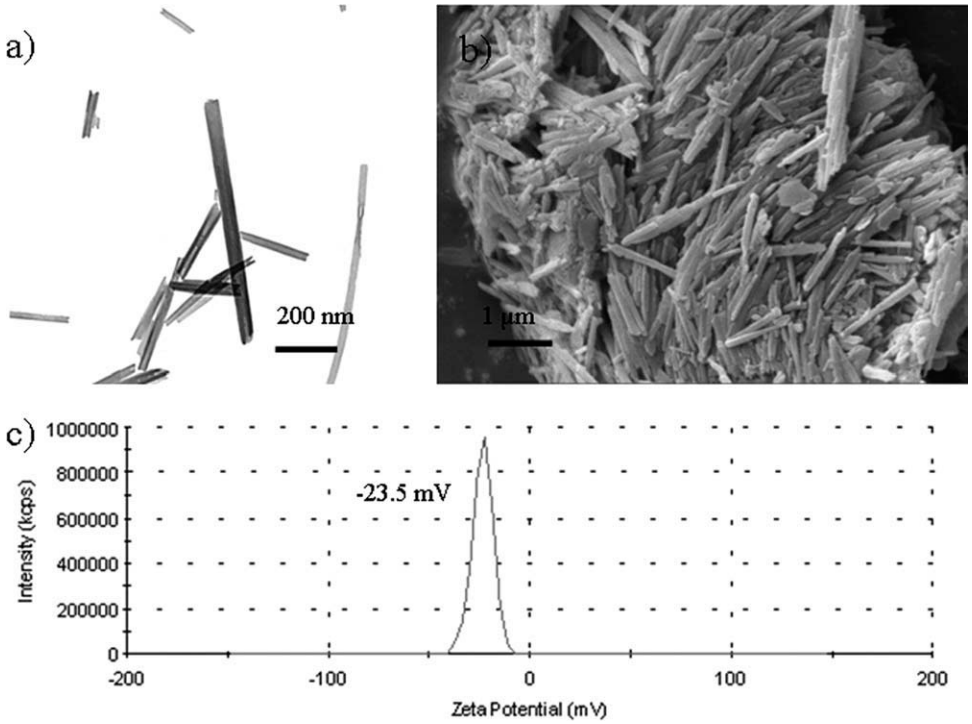

Figure 2 (a) TEM image of HNTs, (b) SEM image of HNTs, (c) Zeta potential obtained using a Malvern Zetasizer for HNTs.

concentration of IBU is linear in our calibration curve established from standard solutions of IBU in PH = 7.4 or 1.2 PBS solution. Each data point was taken from the average of three measurements.

Physicochemical measurement

Gel permeation chromatography (GPC) analysis of the samples was performed at a flow rate of 2.0 mL/min, using polystyrene as standard and 25°C in THF by using Waters 515C equipment. Fourier-transform infrared (FTIR) spectra of the samples were tested on German Vector 33, which was recorded using KBr pellets for solid samples. SEM images were obtained using a ZEISS EVO18 operating at 5–15 kV. All samples were dried on glass substrate and sputter-coated with a thin overlayer of gold to prevent sample-charging effects. EDS was performed on the SEM samples using the EDS function of the SEM. The Pickering emulsion droplets and PLGA microparticle were observed with an optical microscope (Carl Zeiss, German) and the average diameter was estimated by counting 200 beads. Differential Scanning Caborimetry (DSC) curve of the PLGA was obtained using thermo-analyzer (DSC204 F1, NETZCH) with the rate of increasing temperature of 10°C/min. Thermo-gravimetric analysis (TGA) curves of the dry microparticle were collected with a thermo-analyzer (TG 209, NETZCH) within a temperature range of 20–600°C and with the rate of increasing temperature of 10°C/min. The conductivity of the emulsions and the Zeta potential of aqueous HNTs nanoparticles were measured by Malvern Zetasizer Nano ZS90. UV absorbance of IBU was recorded with a Hitachi U-3010 ultraviolet and visible spectrophotometer. Some photos were captured by digital camera (Sony W390).

RESULTS AND DISCUSSION

Characterization of HNTs and PLGA

For this work, HNTs were used as a stabilizer to form Pickering emulsion. HNTs offer great opportunities for fabricating polymer nanocomposites with promising performance.[30–33] HNTs, chemically similar to kaolinite with a molecular formula of $Al_2Si_2O_5(OH)_4{\cdot}nH_2O$, are multiwalled inorganic nanotubes. The tubular halloysite is formed by rolling of a kaolin sheet in preference to tetrahedral rotation to correct the misfit of the octahedral and tetrahedral sheets.[34] Comparing with carbon nanotubes (CNTs), the naturally occurred HNTs are much cheaper and easily available. SEM and TEM[35] observations showed that the HNTs having a 15 nm lumen, 50 nm external diameter, and length of 800 ± 300 nm [see Fig. 2(a,b)]. Zeta potential of this HNTs was −23.5 mV [shown in Fig. 2(c)] obtained using a Malvern Zetasizer.

According to the results of GPC and DSC measurements, we can know M_w (weight-average molecular weight), M_n (Number average molecular weight),

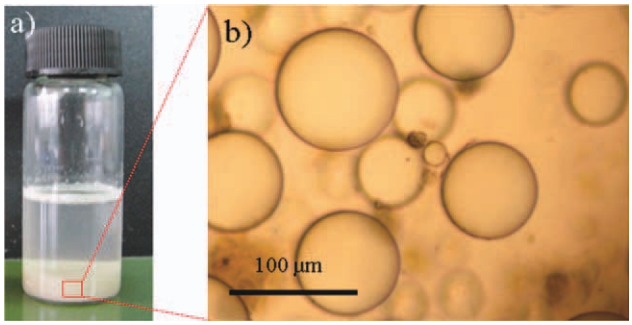

Figure 3 (a) Digital camera photo of the stable emulsion obtained with HNTS 0.5%, (b) optical microscopy image of this emulsion (a). [Color figure can be viewed in the online issue, which is available at wileyonlinelibrary.com.]

PDI (M_w/M_n) and T_g (glass-transition temperature) of PLGA were 18,952 (g/mol), 12,354 (g/mol), 1.53 and 27°C, respectively.

Analysis of emulsion

HNTs-stabilized CH_2Cl_2 solution of PLGA emulsion droplets were prepared in aqueous media in the absence of any molecular surfactant, followed by the evaporation of CH_2Cl_2 leading to HNTs-coated PLGA microparticles. CH_2Cl_2 was selected as a solvent for PLGA because it is inexpensive and relatively volatile and easy to be removed by evaporation. Actually, CH_2Cl_2 has been widely used to fabricate biomaterials.[36–40] In the present study, CH_2Cl_2 solution of PLGA with a molecular weight of 18,952 g/mol and 2.0 wt % solid content was mainly used because the time needed for dissolution in the CH_2Cl_2 is short and a viscosity of the solution is relatively low to allow easy handling.

The conductivity of the emulsions was measured immediately after preparation. And, the conductivity of aqueous nano-composite was 21.4 μS cm^{-1}. It is well known that emulsions were classified according to their conductivities. A high conductivity indicated an oil-in-water emulsion and a low (<1 μS cm^{-1}) conductivity indicated a water-in-oil emulsion. After one week, the stable emulsion was captured by digital camera obtained with HNTs concentration 0.5% [shown in Fig. 3(a)].

A drop of the diluted emulsion or the HNTs-coated PLGA microparticles was placed on a microscope slide and viewed using an optical microscope fitted with a digital camera (Nikon, COOLPIX 4500). This technique was used to estimate the mean droplet in aqueous media and microparticles sizes (n = 200). A typical optical microscopy image of the emulsion was shown in Figure 3(b). The emulsion droplets of CH_2Cl_2 solution of PLGA-in-water were spherical and fairly polydisperse. And, the mean droplet diameter was about 39.8 μm (shown in Fig. 4).

Analysis of the resulting microparticles

When the microparticles were obtained by the evaporation of CH_2Cl_2, and then inspected by both optical microscopy photograph [shown in Fig. 5(c)] and scanning electron microscopy image [shown in Fig. 5(a,b)]. The resulting microparticles sedimented in the aqueous medium with in 20 min due to gravity, if standing still; however, they could easily redisperse in the medium by hand shaking. It was confirmed that the microparticles stored in aqueous medium can redisperse as single microparticles even after several months. The number-average diameter of microparticles became smaller than the diameter of emulsion droplets. This phenomenon should be due to the volume shrinkage with the evaporation of CH_2Cl_2. Figure 5(a,b) showed SEM images of needle-like HNTs coated-microparticles. And, these microparticles maintained a full shape, although these microparticles were damaged during the process of SEM.

The SEM images [Fig. 5(e,f)] revealed that there were well-preserved bare-PLGA microparticles existed on glass substrate. Although these microparticles experienced sputter coated with gold and acid washing, but these bare-PLGA microparticles still keep good shapes. So we can demonstrate that these bare-PLGA microparticles are surely robust and strong. Optical microscopy images of bare-PLGA microparticles can also exhibit good shape, shown in Figure 5(g).

Figure 5(d,h) shows the EDS spectra obtained for the microparticles without acid aqueous solution treatment and with acid aqueous solution treatment, respectively. The sample without acid aqueous solution treatment showed some prominent silicon, aluminum peaks at 1.75 keV, 1.45 keV apart from the oxygen and carbon peaks at 0.5 and 0.2 keV, respectively. Whereas, the silicon and aluminum peaks

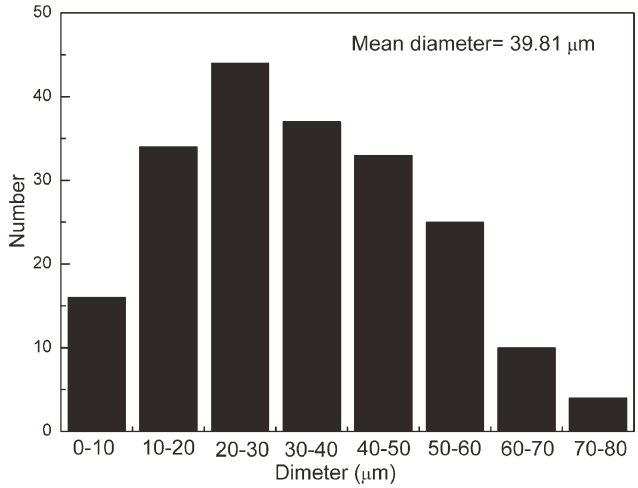

Figure 4 Size distribution graph, (n = 200).

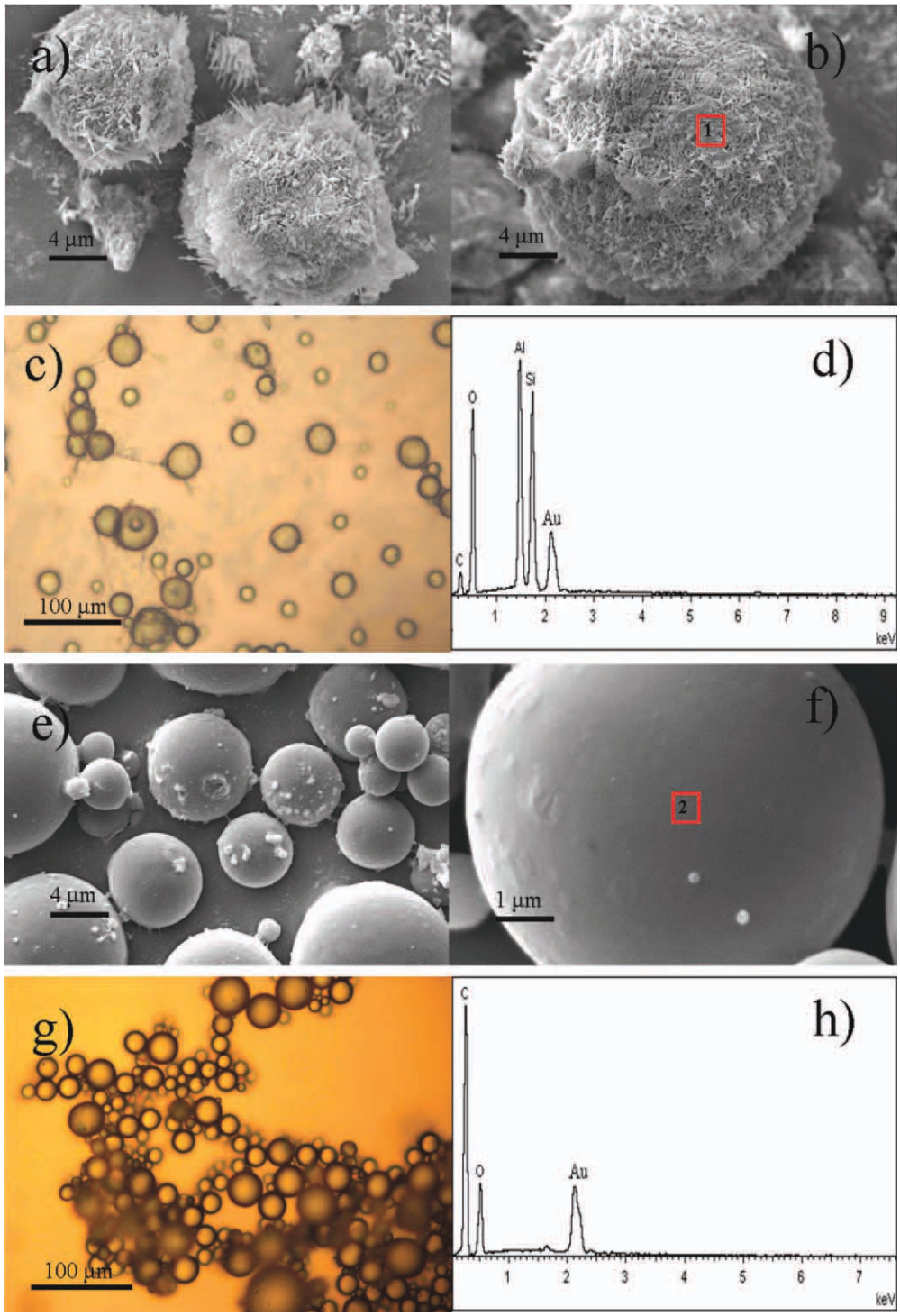

Figure 5 SEM images of microparticles, (a), (b) HNTs-coated PLGA microparticles; (e), (f) bare-PLGA microparticles. (d), (h) EDS spectra of the hybrid microparticle and bare-PLGA micro-particle at area 1 in Figure 5(b) and area 2 in Figure 5(f), respectively. Optical microscopy microscopy images of HNTs-coated PLGA microparticles (c) and bare-PLGA micro-particles (g). [Color figure can be viewed in the online issue, which is available at wileyonlinelibrary.com.]

were virtually absent in the EDS spectra obtained for the microparticles with acid aqueous solution treatment. It is well known that the strong peaks of silicon and aluminum come from the HNTs, and the apparent peaks of C, O could be attributed to the PLGA in the microparticles structure. So the EDS results indicated that most of HNTs were removal from the microparticles during the process of acid aqueous solution treatment. Moreover, if the HNTs were enveloped in the PLGA microparticles, acid aqueous solution treatment could not remove them. However, the EDS spectrum of Figure 6(h) showed

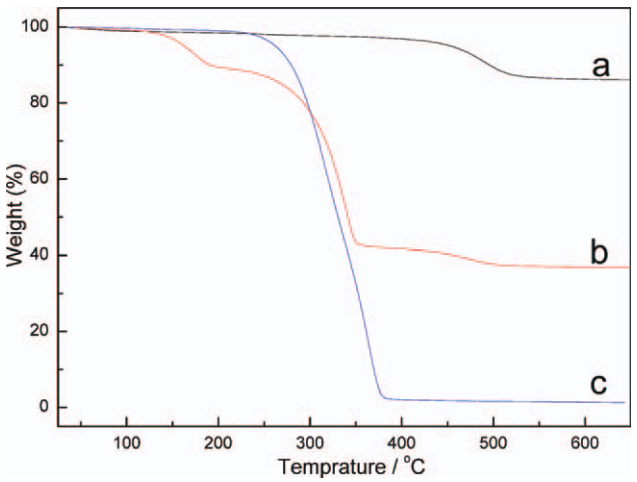

Figure 6 T_g curves of (a) HNTs, (b) HNTs-coated PLGA microparticles, (c) bare-PLGA microparticles (after washing with acid). [Color figure can be viewed in the online issue, which is available at wileyonlinelibrary.com.]

that there was no silicon and aluminum in the bare-PLGA microparticles. In general, HNTs could only covered on the surface of the microparticles. The atomic percentage of silicon (shown in Table III) in the microparticles decreased from 7.17 to 0%, and the change of aluminum is the same as silicon. So the resulting microparticles were only PLGA-microparticles, which is suitable to biocompatible engineering.

The dry microparticles were analyzed by TGA to determine PGLA and HNTs contents. The weight loss in HNTs, HNTs-coated PLGA microparticles, and bare-PLGA microparticles were 13.48, 62.57, and 98.8%, respectively (shown in Fig. 6). From Figure 6(a), weight loss of 13.48% was attributed to the combined water and hydroxyl from the HNTs. As shown in Figure 6(b), when temperature was raised to ca. 160°C, weight loss of this section was attributed to an elimination of remnant water from the HNTs. Subsequently, there was a strong weight loss from ca. 250 to 400°C due to the degradation of PLGA chains. Finally, there was a little weight loss from ca. 400 to 500°C due to the condensation of hydroxyl in HNTs. In Figure 6(c), weight loss of 98.8% was mainly attributed to the thermal decomposition of PLGA. Thus, after washing with acid aqueous solution, the remnant percentage of HNTs in the microparticles decreased from 37.43% to negligibly small amount of 1.2%. In general, the result of TGA is coincident with the EDS analyses.

TABLE III
EDS Results of Microparticles

	HNTs-coated PLGA microspheres		Bare PLGA microparticles	
Entry	Percentage by weight (%)	Percentage by atom (%)	Percentage by weight (%)	Percentage by atom (%)
C	18.30	27.41	19.23	24.07
O	57.68	58.01	80.77	75.93
Si	11.53	7.17	0	0
Al	12.49	7.41	0	0

To confirm the HNTs existence or absence in microparticles, FTIR studies were conducted (see Fig. 7). In the FTIR spectrum of the pure HNTs [Fig. 7(a)], the peaks at 910 cm^{-1} and 1031 cm^{-1} are attributed to the absorbance of Al—O and Si—O in HNTs, respectively. In the spectrum of this pure PLGA [Fig. 7(b)], the peaks at 1761 cm^{-1} is attributed to the absorbance of C=O in PLGA matrix. In Figure 7(c), the peaks at 1761 and 1031 cm^{-1} are ascribed to the absorbance of C=O in PLGA and Si—O in HNTs, respectively. In bare-PLGA microparticles washed by acid aqueous solution, the typical peaks appeared at 1761 cm^{-1} still exist, but the peak at 1031 and 910 cm^{-1} are nearly disappeared, as was expected [see Fig. 7(d)]. According to the results of the IR spectra analysis, the synthesis of HNTs-coated PLGA microparticles and bare-PLGA microparticles are successful. Overall, the result acts in accordance with EDS and TGA analyses.

Analysis of loading capacity and encapsulation efficiency

Drug-loading and encapsulation efficiency are important indices for drug delivery systems. This is especially true for expensive drugs. IBU of poor water-solubility was dispersed in the CH_2Cl_2 solution of PLGA by stirring and ultrasonication. With the evaporation of CH_2Cl_2 from the emulsion, most

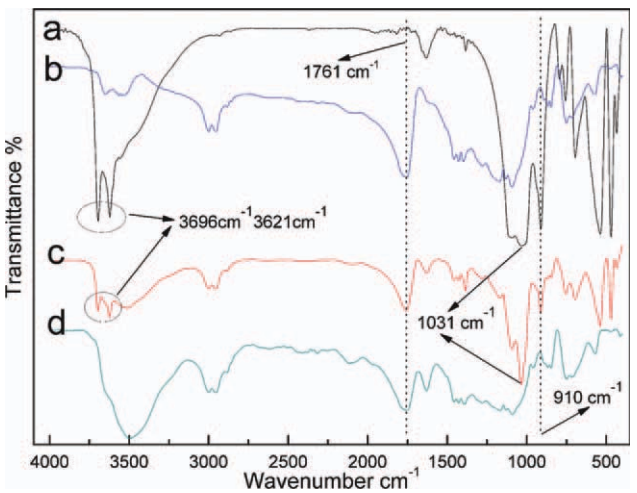

Figure 7 FTIR spectra of (a) HNTs, (b) pure PLGA, (c) HNTs-coated PLGA microparticles, (d) bare-PLGA microparticles. [Color figure can be viewed in the online issue, which is available at wileyonlinelibrary.com.]

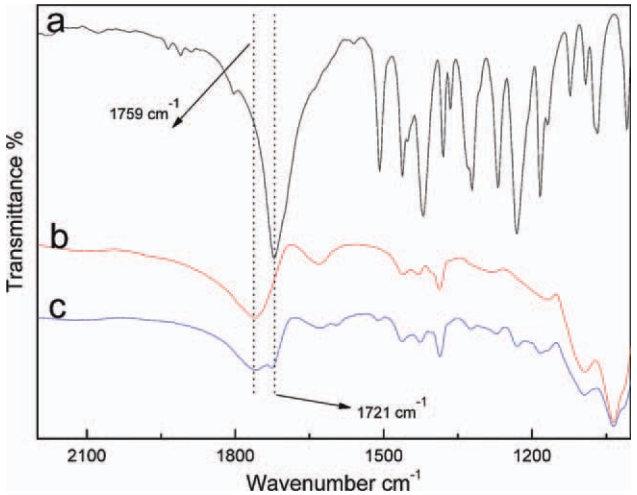

Figure 8 FTIR spectra of (a) pure IBU, (b) HNTs-coated PLGA microparticles. (c) IBU encapsulated in HNTs-coated PLGA microparticles. [Color figure can be viewed in the online issue, which is available at wileyonlinelibrary.com.]

of IBU was encapsulated in PLGA microspheres, and then a little of unencapsulated IBU released into water (continues phase). To confirm the IBU existence or absence in bare PLGA microparticles, FTIR studies were conducted (see Fig. 8). In the FTIR spectra of the IBU [Fig. 8(a)], the peaks at 1721 cm^{-1} are attributed to the absorbance of C=O in IBU. In the spectrum of this pure PLGA [Fig. 8(b)], the peaks at 1760 cm^{-1} is attributed to the absorbance of C=O in PLGA matrix. In Figure 8(c), the peaks at 1760 and 1721 cm^{-1} are ascribed to the absorbance of C=O in PLGA and C=O in IBU, respectively. According to the results of the IR spectra analysis, it can be proved that IBU was successfully encapsulated in bare PLGA microparticles.

Drug loading content and encapsulation efficiency were determined using UV–vis method. The results are shown in Table II, each data point in this table is represents the average of three tests, $n = 3$. Reasonable loading and encapsulation efficiency were obtained using water solution (pH = 7.2, 5, 3, 1) with drug loading of 5.42–29.35%, and encapsulation efficiency of 76.51–97.83%. The pH value in the water solution had dramatically affected on the IBU loading capacity and encapsulation efficiency. In Figure 9(a), DL% and EE% decreased with the increase of the pH value. This reason is that protonation and deprotonation of IBU at different pH value would affected on the solubility of IBU. In addition, DL% and EE% would increase by increasing the ratio of IBU and PLGA [shown in Fig. 9(b)], because IBU was a poor water-solubility drug. It is worth while to mention that the morphology and characteristic size of PLGA microparticles remain unchanged after IBU is loaded, observed by optical microscope.

In vitro release study

IBU is the most widely used as a clinical drug. The research on IBU delivery and release has attracted many interests, including oral IBU delivery. IBU as a drug model was loaded into the bare-PLGA microparticles by dispersing in the PLGA-CH_2Cl_2 solutions before evaporation of CH_2Cl_2. After removal of CH_2Cl_2, the IBU was stored in a closed PLGA microparticle. They could be easily redispersed in water and keep spherical after storage for more than a month. The release behavior of IBU from the bare-PLGA microparticles was investigated. The release profile at pH 7.4 and 1.2 was shown in Figure 10, each data point on this graph is represents the average of three tests, $n = 3$. This release pattern is typical of release of macromolecules from PLGA microspheres.[41,42] Because of a better solubility at pH 7.4 than at pH 1.2, the releases of IBU in bare-PLGA microparticle at pH 7.4 is faster than at pH 1.2. Because of the same reason as mentioned above, the total accumulative IBU release is 71.26% at pH 7.4 [shown in Fig. 10(a)], more than 42.96% at pH 1.2

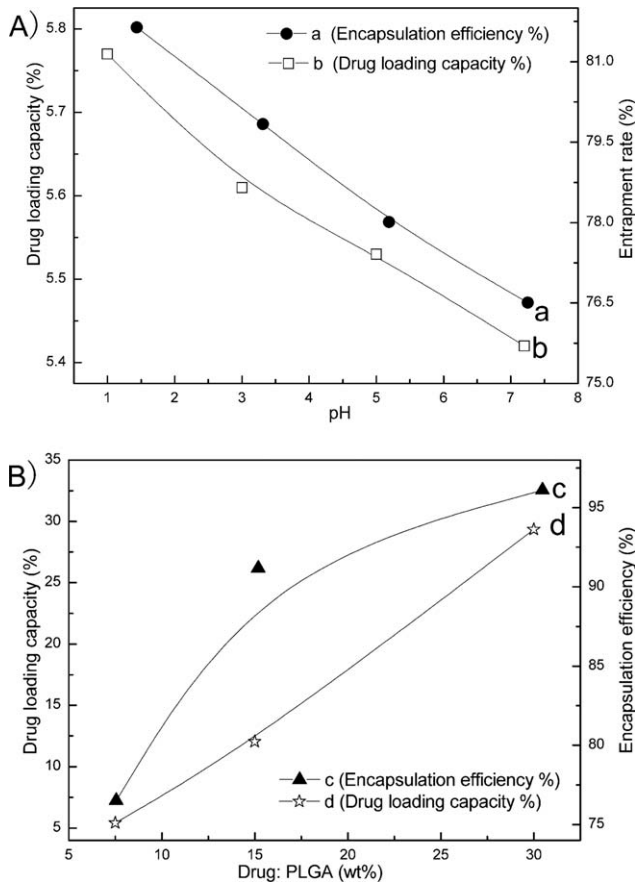

Figure 9 (A) pH value of PBS solution has a dramatical affect on EE% (a) and DL% (b). (B) And, wt% of drug in PLGA has a strong impact on EE% (c) and DL% (d). Each point on this graph is represents the average of three tests ($n = 3$).

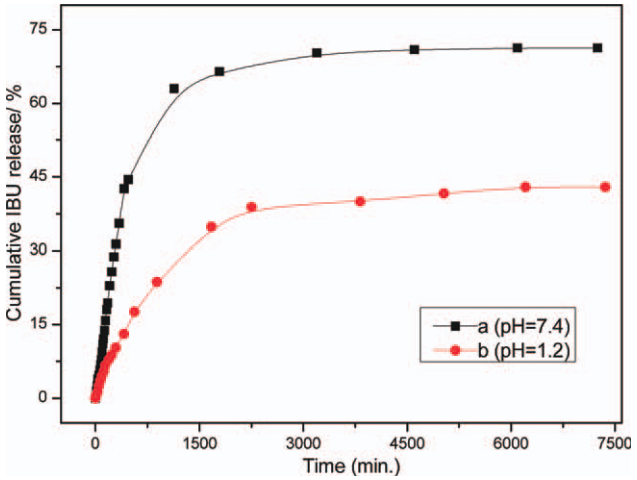

Figure 10 Release curve at pH 7.4 and 1.2 of bare PLGA microparticles loaded IBU. Each point on this graph is represents the average of three tests ($n = 3$). [Color figure can be viewed in the online issue, which is available at wileyonlinelibrary.com.]

[shown in Fig. 10(b)]. Release of the drug is relatively rapid in the first stage (0–2000 min) followed by a gradual decrease in release rate over a study period. The initial rapid release of the drug is most likely due to the release of drug on the surface and near the exterior surface.[42] IBU continued to be released from bare PLGA microparticle at a slower rate for over 3000 min, after which the release rate was minimal. Because of the barrier of the polymeric matrix (PLGA), some IBU was tightly encapsulated in the core of the bare PLGA microparticle. So these IBU (28.74% at pH 7.4 and 57.04% at pH 1.2) would release with the disintegrate of the bare PLGA microparticle in future.

To describe the kinetics of drug release and the discernment of the release mechanisms, we use the Higuchi law, Weibull equation, First-order kinetic equation and the Hixcon-Crowell model[43–46] to fit the curve of IBU release from the bare PLGA microparticle at different pH value. The Higuchi law indicates that the fraction of drug released is proportional to the square root of time

$$\frac{M_t}{M_\infty} = kt^{1/2} \tag{3}$$

where M_t/M_∞ is the fractional drug released at time t, M_t and M_∞ are cumulative amounts of drug released at time t and infinite time, and k is a constant related to the formulation of loaded drug and release medium. The Weibull equation is expressed as:

$$\frac{M_t}{M_\infty} = 1 - \exp(-at^b) \tag{4}$$

where a and b are constants. Although this function is frequently applied to the analysis of dissolution and release studies, its empirical use has been criticized.[47] Recently, Kosmidis et al. found that eq. (4) describes nicely the entire drug release curve of release from the spherical matrices.[48] Here the Higuchi law can be predigested as:

$$F = kt^{1/2} \tag{5}$$

The Weibull equation can be expressed as:

$$LnLn\left[\frac{1}{1-F}\right] bLnt + Lna \tag{6}$$

where F is M_t/M_∞, the fractional drug released at time t.

The Hixcon-Crowell model can be expressed as:

$$(1-F)^{1/3} = b + k(t - L_{app}) \tag{7}$$

where F is M_t/M_∞, the fractional drug released at time t. b and k are constants related to this model. By definition, L_{app} is a particular time, when the cumulative amounts of drug released reached 10%.

The First-order kinetic equation is expressed as:

$$F = 1 - \exp(kt) \tag{8}$$

where F is M_t/M_∞, the fractional drug released at time t. k is constant related to this equation.

We fit the IBU release curves for the bare PLGA particles at pH 7.4 and pH 1.2 using eqs. (5)–(8). The value of r which is the correlation coefficient of the linear regressions is listed in Table IV. From Table IV, we can see that the values of r derived from the linear regressions of the Weibull equation are very close and larger than that from the linear regressions of other equations. Thus the Weibull equation can better fit the IBU release curves. The good fitting curves and regression lines by eq. (6) to the releases from the bare PLGA microparticles at pH 1.2 and pH 7.4 are shown in Figure 11.

It is well known that the slope of the regression line of eq. (6) is the constant b of Weibull equation.

TABLE IV
The Correlation Coefficients of The Linear Regressions of Fitting Release Curves by Different Models

Model	Bare PLGA microparticles (r)	
	pH = 7.4	pH = 1.2
First-order kinetic equation	−0.85095	−0.89827
Higuchi	0.90899	0.9634
Weibull	0.95427	0.98264
Hixcon-Crowell	−0.83319	−0.89217

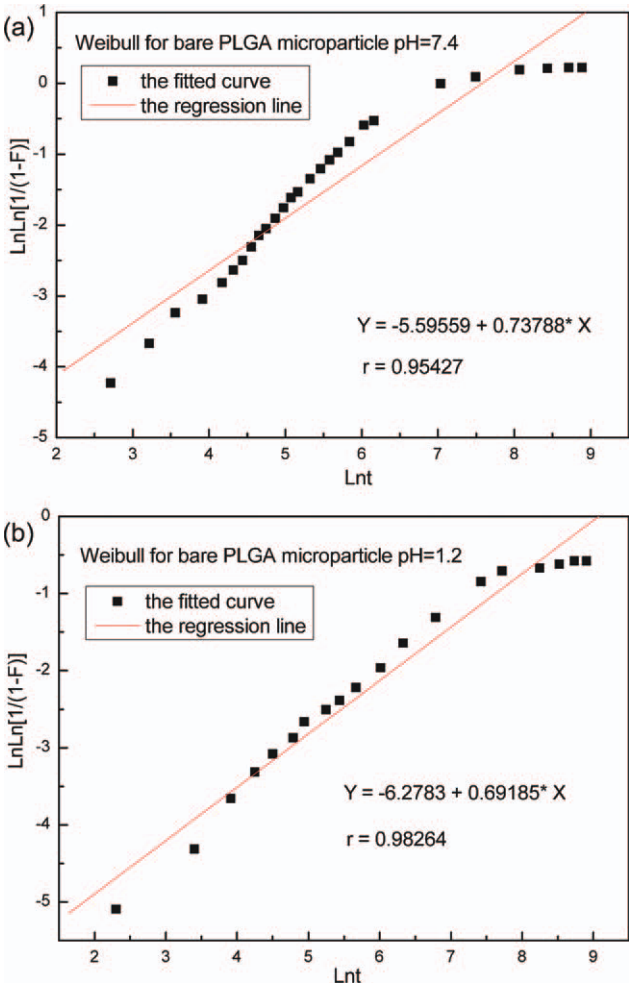

Figure 11 The fitting regression line by Weibull equation for IBU release from the bare PLGA microparticles at pH 7.4 (a), pH 1.2 (b). [Color figure can be viewed in the online issue, which is available at wileyonlinelibrary.com.]

From Figure 11, *b* for the bare PLGA microparticles at pH 1.2, and 7.4 is 0.69 and 0.74, respectively. Kosmidis et al. concluded that Weibull equation arises from the creation of a concentration gradient near the releasing boundaries of the Euclidian matrix or because of the "fractal kinetics" behavior associated with the fractal geometry of the environment.[49] They also summarized the diffusional mechanism in connection with the specific *b* values of Weibull equation and concluded that for values of b lower than 0.75 the release follows Fickian diffusion and for Fickian diffusion the increase of *b* reflects the decrease of the disorder of the medium. In general, Weibull equation can nicely fit the IBU release curves and the release follows Fickian diffusion.

CONCLUSIONS

In this study, well-defined nanocomposite PLGA microparticles and bare PLGA microparticles were easily prepared by self-assembly of HNTs particles at liquid–liquid interfaces and subsequent in situ evaporation with an approximate 100% yield, which is promising to produce in large quantity for industry. Halloysite as a particular emulsifier in Pickering emulsion was firstly reported. And, halloysites are cheap, abundantly available, and durable and biocompatible.

This strategy was fabricated via a combined system of "Pickering-type" emulsion route and solvent volatilization method in the absence of any molecular surfactants. And the biocompatible bare-PLGA microparticles should be useful for a variety of biomedical applications including drug delivery system, cell carrier, and scaffold, because these microparticles can be loaded with drug or reagent. The release curve can be nicely fitted by the Weibull equation and the release follows Fickian diffusion. This method for synthesis of nanocomposite and biocompatible microparticles described here offers potential advantages over polymerization route using Pickering-type monomer droplets.[50,51] These include application of wider range of polymers (vinyl and nonvinyl polymers), easier incorporation of functional chemicals such as drugs, and easier conduction which needs no special apparatus. The combined system used in this paper will open up a new route to the preparation of a variety of drug-carrying microparticles.

References

1. Qi, Y.; Li, N. J.; Xu, Q. F.; Ge J. F; Xia, X. W.; Lu J. M. J Appl Polym Sci 2011, 121, 2843.
2. Oledzka, E.; Kong, X.; Narine S. S. J Appl Polym Sci 2011, 119, 1848.
3. Sahoo, S.; Sasmal, A.; Sahoo, D.; Nayak, P. J Appl Polym Sci 2010, 118, 3167.
4. Aveyard, R.; Binks, B. P.; Clint, J. H. Adv Colloid Interface Sci 2003, 100–102, 503.
5. Fujii, S.; Okada, M.; Sawa, H.; Furuzono, T.; Nakamura, Y. Langmuir 2009, 25, 9759.
6. Liu, X. W.; Okada, M.; Maeda, H.; Fujii, S.; Furuzono, T. Acta Biomater 2011, 7, 821.
7. Ramsden, W. Proc Roy Soc 1903, 72, 156.
8. Aveyard, R.; Binks, B. P.; Clint, J. H. Adv Colloid Interface Sci 2003, 503, 100.
9. Binks, B. P.; Lumsdon, S. O. Langmuir 2000, 16, 2539.
10. Yin, D. Z.; Zhang, Q. Y.; Yin, C. J.; Jia, Y.; Zhang, H. P. Colloids Surf A, 2010, 367, 70.
11. Huang, J. J.; Pen, H.; Xu, Z. S.; Yi, C. F. Reac Funct Polym 2008, 68, 332.
12. Wang, C. Y.; Zhang, C. J.; Li, Y.; Chen, Y. H.; Tong, Z. Reac Funct Polym 2009, 69, 750.
13. Do, T.-A. L.; Mitchell, J. R.; Wolf A. B.; Vieira, J. Reac Funct Polym 2010, 70, 856.
14. Fujii, S.; Okada, M.; Furuzono, T. J. J. Colloid Interface Sci 2007, 315, 287.
15. Fujii, S.; Okada, M.; Sawa, H.; Furuzono, T.; Nakamura, Y. Langmuir 2009, 25, 9759.
16. Bon, S. A. F.; Colver, P. J. Langmuir 2007, 23, 8316.

17. Chen, J.; Vogel, R.; Werner, S.; Heinrich, G.; Clausse, D.; Dutschk, V. Colloids Surf A 2011, 382, 238.
18. Wang, J.; Liu, G. P.; Wang, L. Y.; Li, C. F.; Xu, J.; Sun, D. J. Colloids Surf A 2010, 353, 117.
19. Muller, F.; Salonen, A.; Glatter, O. Colloids Surf A 2010, 358, 50.
20. Fujii, S.; Read, E. S.; Armes, S. P.; Binks, B. P. Adv Mater 2005, 17, 1014.
21. Binks, B. P.; Lumsdon, S. O. Langmuir 2001, 17, 4540.
22. Reis, B. M.; Armes, S. P.; Fujii, S.; Biggs, S. Colloids Surf A 2010, 353, 210.
23. Lvov, Y. M.; Shchukin, D. G.; Möhwald, H.; Prince, R. R. ACS Nano 2008, 2, 814.
24. Vergaro, V.; Abdullayev, E.; Lvov, Y. M.; Zeitoun, A.; Cingolani, R.; Rinaldi, R.; Leporatti, S. Biomacromolecules, 2010, 11, 820.
25. Athanasiou, K. A.; Niederauer, G. G.; Agrawal, C. M. Biomaterials 1996, 17, 93.
26. Rezwan, K.; Chen, Q. Z.; Blaker, J. J. Biomaterials 2006, 27, 3413.
27. Wong, J.; Brugger, A.; Khare, A.; Chaubal, M.; Papadopoulos, P.; Rabinow, B.; Kipp, J.; Ning, J. Adv Drug Deliv Rev 2008, 60, 939.
28. Menner, A.; Verdejo, R.; Shaffer, M.; Bismarck, A. Langmuir 2007, 23, 2398.
29. Shchukin, D. G.; Sukhorukov, G. B.; Price, R. R.; Lvov, Y. M. Small 2005, 1, 510.
30. Ning, N. Y.; Yin, Q. J.; Luo, F.; Zhang, Q.; Du, R. N.; Fu, Q. Polymer 2007, 48, 7374.
31. Du, M. L.; Guo, B. C.; Liu, M. X.; Jia, D. M. Polym J 2007, 39, 208.
32. Du, M. L.; Guo, B. C.; Jia, D. M. Eur Polym J 2006, 42, 1362.
33. Liu, M. X.; Guo, B. C.; Du, M. L.; Cai, X. J.; Jia, D. M.; Nanotechnology 2007, 18, 455703.
34. Singh, B. Clays Clay Miner 1996, 44, 191.
35. Liu, M. X.; Guo, B. C.; Zou, Q. L.; Du, M. L.; Jia, D. M. Nanotechnology 2008, 19, 205709.
36. Jeffery, H.; Davis, S. S.; O'Hagan, D. T. Int J Pharm 1991, 77, 169.
37. Verrecchia, T.; Huve, P.; Bazile, D.; Veillard, M.; Spenlehauer, G.; Couvreur, P. J. Biomed Mater Res 1993, 27, 1019.
38. Kim, H. W.; Lee, H. H.; Knowles, J. C. J Biomed Mater Res A 2006, 79, 643.
39. Khil, M. S.; Bhattarai, S. R.; Kim, H. Y.; Kim, S. Z.; Lee, K. H. J Biomed Mater Res B: Appl Biomater 2005, 72, 117.
40. Luong-Van, E.; Gro endahl, L.; Chua, K. N.; Leong, K. W.; Nurcombe, V. S. M. Cool Biomaterials 2006, 27, 2042.
41. Tambe, D. E.; Sharma, M. M. Adv Colloid Interface Sci 1994, 52, 1.
42. Alonso, M. J.; Cohen, S.; Park, T. G.; Gupta, R. K.; Siber, G. R.; Langer, R. Pharm Res 1993, 10, 945.
43. Wang, H. T.; Schmitt, E.; Flanagan, D. R.; Linhardt, R. J. J Control Release 1991, 17, 23.
44. Higuchi, T. J Pharm Sci 1961, 50, 874.
45. Vooren, L. V.; Krikilion, G.; Rosier, J.; Spiegeleer, B. D. Drug Dev Ind Pharm 2001, 27, 885.
46. Weibull, W. J. Appl Mech 1951, 18, 293.
47. Costa, P.; Sousa Lobo, J. M. Eur J Phrarm Sci 2001, 13, 123.
48. Kosmidis, K.; Argyrakis, P.; Macheras, P. Pharm Res 2003, 20, 988.
49. Papadopoulou, V.; Kosmidis, K.; Vlachou, M.; Macheras, P. Int J Pharm 2006, 309, 44.
50. Gao, Q. X.; Wang, C. Y.; Liu, H. X.; Wang, C. H.; Liu, X. X.; Tong Z. Polymer, 2009, 50, 2587.
51. Liu, H. X.; Wang, C. Y.; Gao, Q. X.; Liu, X. X.; Tong, Z. Acta Biomaterialia 2010, 6, 275.